



Scaling relation for occulter manufacturing errors

Dan Sirbu^{1,3}, Stuart B. Shaklan², N. Jeremy Kasdin¹, Robert J. Vanderbei¹
¹Princeton University, ²NASA JPL, ³NASA ARC

OBJECTIVE

For directly imaging exoplanets, NASA is considering space mission designs that use an external occulter as the principal starlight suppression system. These occulter designs range in diameter from 16 to 40 m and separation distance from 8,000 to 60,000 km for telescopes with primary diameters of 0.5 to 4 m (1-2).

Occluter shapes are solutions to an optimization problem (3) which seeks to maximize suppression in the shadow subject to constraints such as size, separation, and wavelengths. These designs are based on scalar diffraction theory and must be verified experimentally to demonstrate predicted on-orbit performance. Due to the large sizes and separations involved the experiment must be scaled to lab size (4-5).

We are currently expanding the existing experimental testbed at Princeton to enable scaling of occulters operating at flight Fresnel sizes. Here we examine the effect on suppression performance of edge defects and their scaling to testbed size.

OCCULTER SCALING

For a plane wave incident on the space occulter, the electric field downstream at the telescope can be computed assuming an apodization function $A(r)$:

$$E_o(\rho) = E_0 e^{jkz} \left(1 - \frac{k}{jz} \int_0^R e^{\frac{jk}{2z}(r^2 + \rho^2)} J_0 \left(\frac{kr\rho}{z} \right) A(r) r dr \right)$$

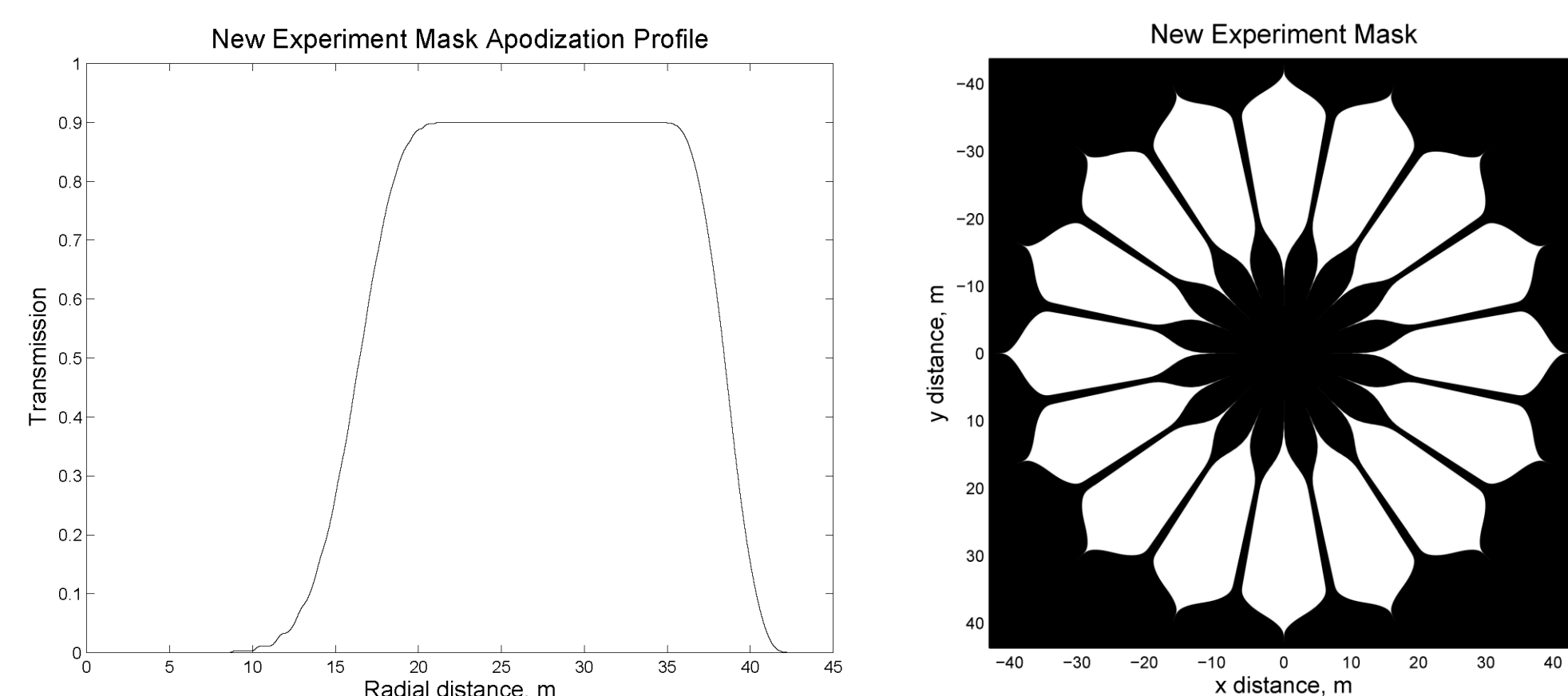
We can introduce scaling relationships that maintain the Fresnel numbers $r^2 / \lambda z$ and $\rho^2 / \lambda z$ constant via a scaling factor a :

$$E_o(\rho) = E_0 e^{kjz} a^2 \left(1 - \frac{k}{jz'} \int_0^{R'} A(ar') J_0 \left(\frac{kr'\rho'}{z'} \right) e^{\frac{jk}{2z'}(r'^2 + \rho'^2)} r' dr' \right)$$

where in the above $\rho' \rightarrow \rho/a$, $r' \rightarrow r/a$, and $z' \rightarrow z/a^2$

MASK DESIGN

We compare the design of the space occulter with other existing designs. We also design an outer ring to minimize the diffraction effects from a finite-size:



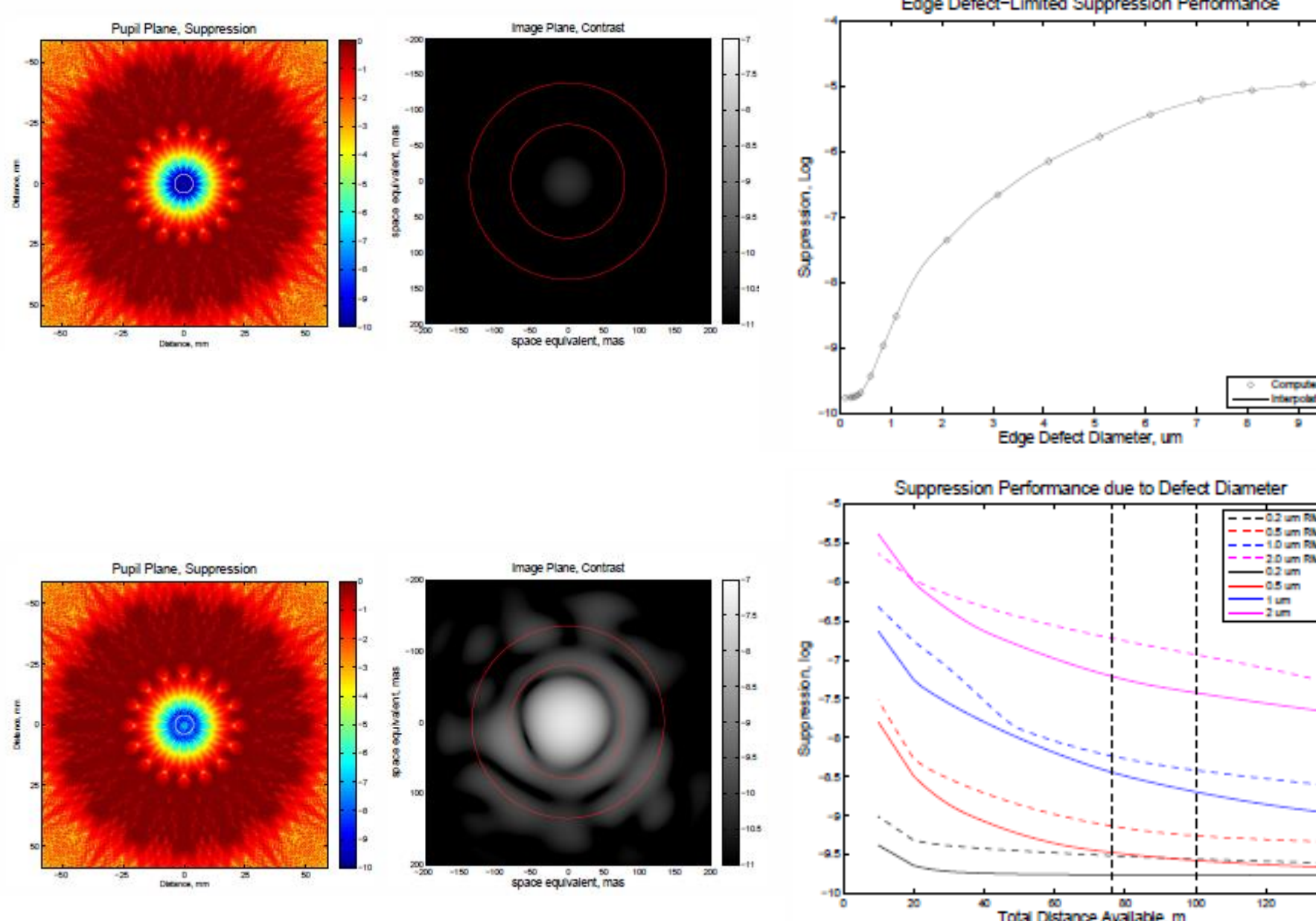
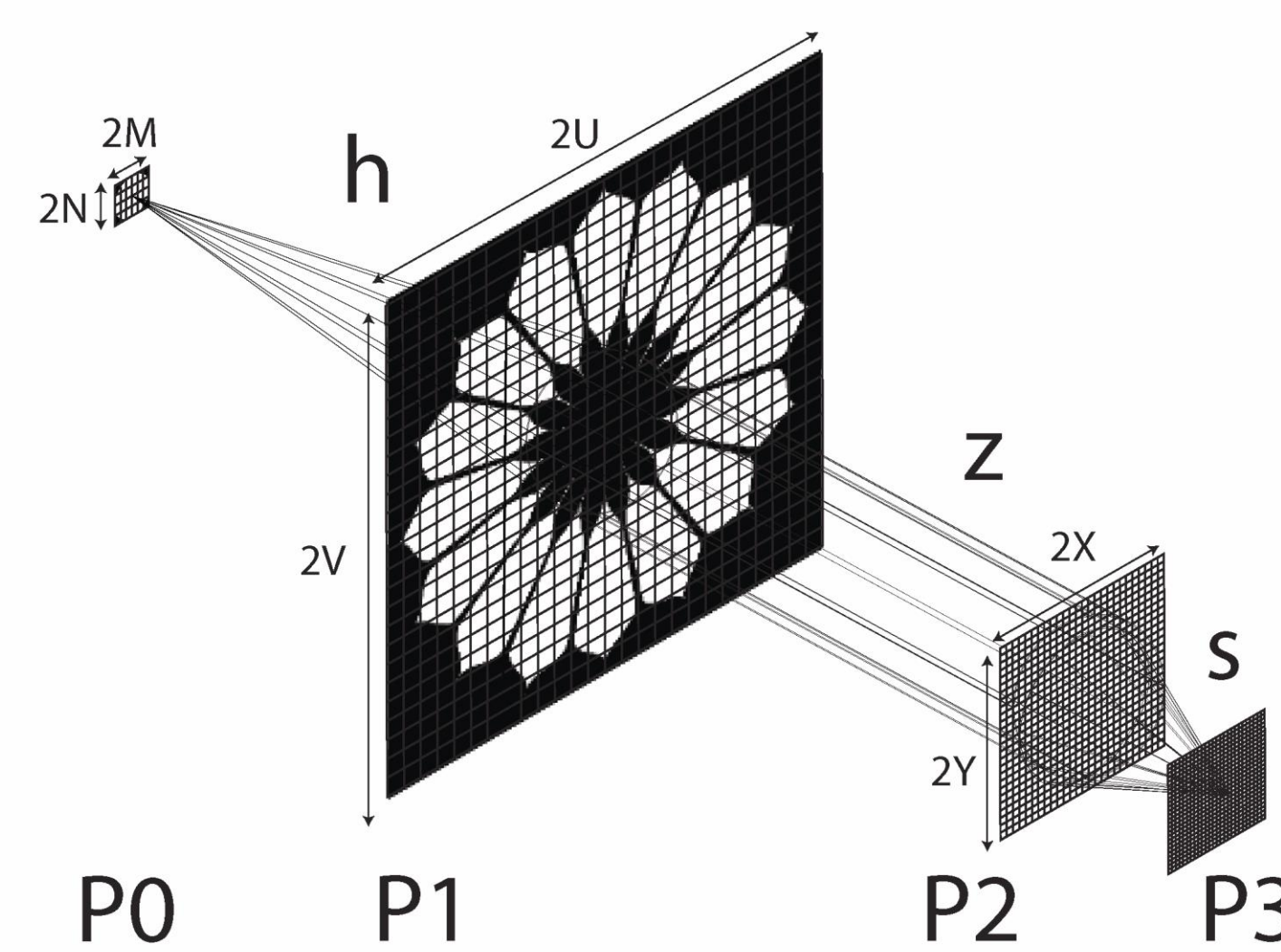
Design	Occluter Radius, R	Separation, z	Wavelength, λ	Fresnel Number
THEIA	20m	55,000 km	600 nm	12.1
O3	17m	19,500 km	600 nm	24.7
Current Experiment	188 m	97,000 km	600 nm	607.3
Extended Experiment	21.9 m	55,000 km	600 nm	14.5

Our testbed uses a diverging input beam to minimize optics aberrations. The occulter mask is placed at half-way of the total available distance to maximize its size.

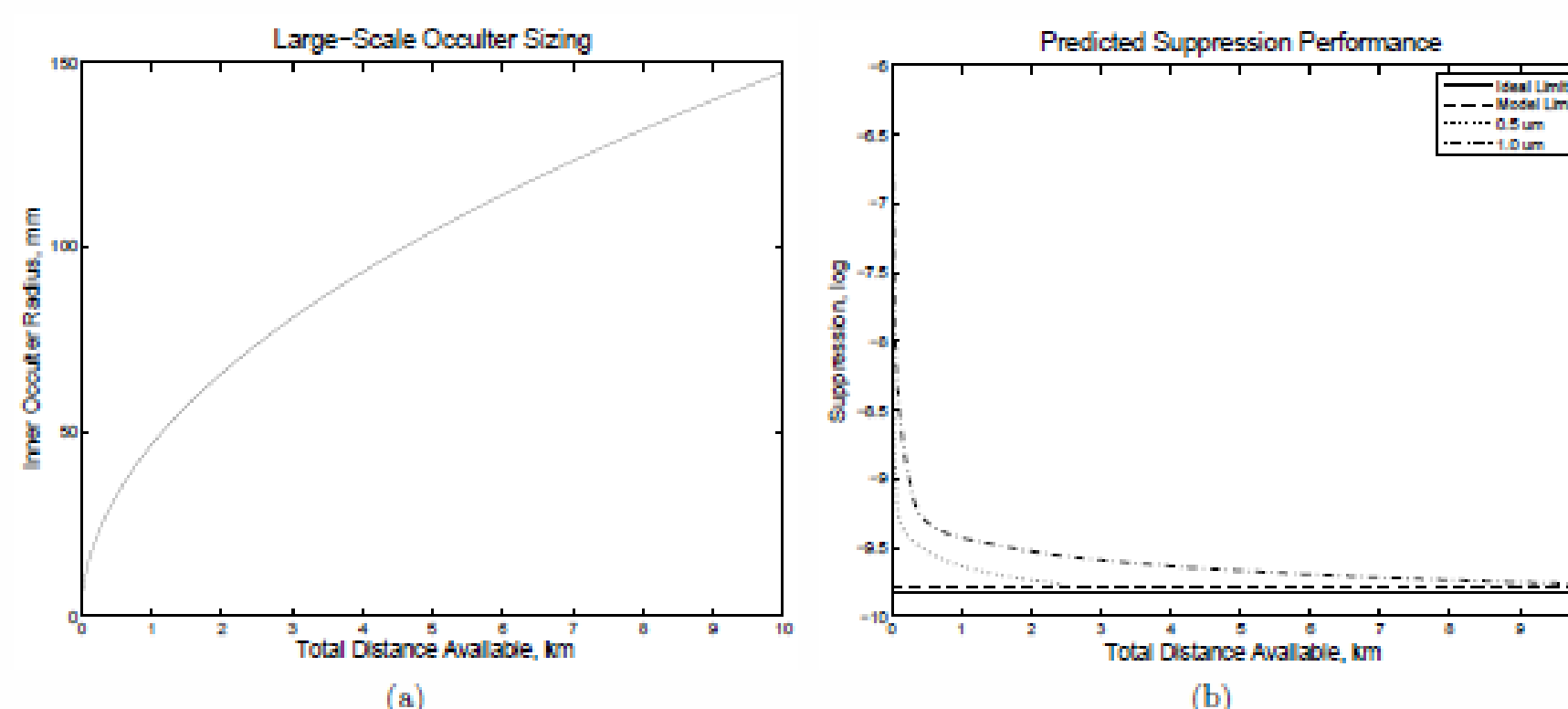
Parameter	Space Design	Collimated Scale	Diverging Scale	
Separation distance, z	55,000 km	38 m	50 m	38 m
Distance scale, a	1	1200	1050	1200
Source distance, h	∞	∞	38 m	50 m
Divergence scale, γ	1	1	1.4	1.4
Inner radius, R_{in}	21.9 m	18.2 mm	20.8 mm	12.8 mm
Outer radius, R_{out}	43.7 m	36.4 mm	41.7 mm	25.8 mm
Dark shadow radius, ρ_{dark}	2.6 m	2.2 mm	2.5 mm	3.1 mm
Outer shadow radius, ρ_{out}	43.7 m	36.4 mm	41.7 mm	57.8 mm
Telescope diameter, D	4 m	3.3 mm	3.8 mm	3.3 mm

OPTICAL PROPAGATIONS

We use a 2D diffraction model first developed in (6) to perform a sensitivity analysis for determining the effect of laboratory-environment errors such as finite feature sizes and tunnel-induced diffraction effects.



(Left) Sample propagations for increasing feature sizes (Right) Fitting of computed feature sizes for different propagation distances

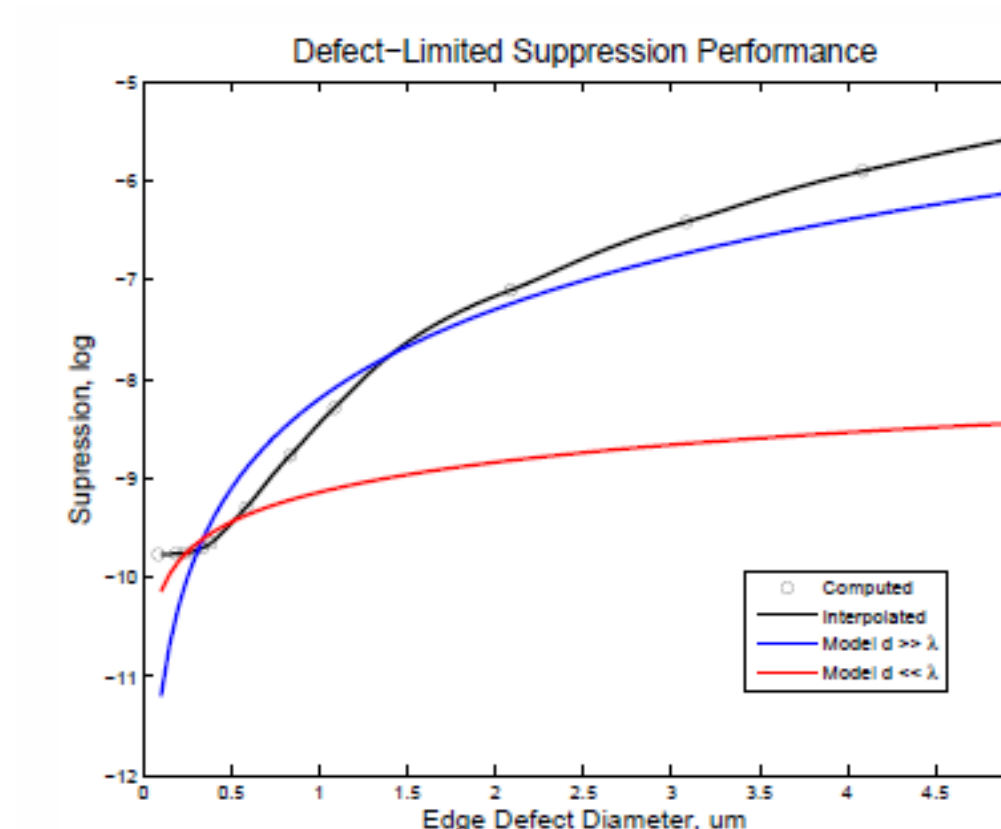
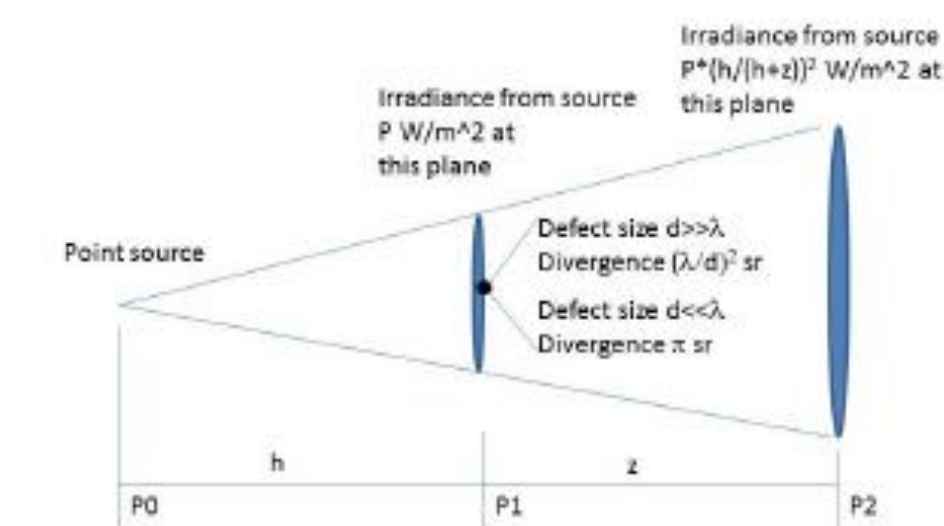


ANALYTICAL MODEL

The ratio of the pupil plane energy received from defects to the energy received from the point source is the suppression limit given for two cases depending on defect size with respect to wavelength of light

$$R = \frac{4Ld^3}{(\lambda h)^2}, \quad d \gg \lambda$$

$$R = \frac{Ld(h+z)^2}{\pi(hz)^2}, \quad d \ll \lambda$$



Comparison of the computed suppression performance for circular defects vs. the analytical model

We can thus model the expected effect on the performance of the occulter edge defects.

CONCLUSIONS

An optimized occulter mask was designed for realistic space mission parameters. This was then scaled to a laboratory size maintaining a constant Fresnel number. Optical propagations were performed that verified the suppression and contrast performance under scaling for finite feature sizes, and also the effect of random manufacturing errors along the petal edges.

We have also developed an analytical model that can be used to more easily ascertain the effect of defects without using the full optical propagations.

REFERENCES

- (1) NJ Kasdin et al. A Telescope for Habitable Exoplanets and Interstellar/Intergalactic Astronomy. White Paper, 2009.
- (2) NJ Kasdin et al. O3: The Occulting Ozone Observatory. AAS 2010.
- (3) RJ Vanderbei et al. Optimal occulter design for finding extrasolar planets. ApJ, 2007, Vol. 665.
- (4) E Cady. Design, Tolerancing, and Experimental Verification of Occulters for Finding Extrasolar Planets. PhD thesis.
- (5) D Sirbu et al. "Monochromatic verification of high-contrast imaging with an occulter," *Optics Express* 21(26), 2013
- (6) D Sirbu et al. "Diffraction analysis of limits of an occulter experiment," *Proc. SPIE, Vol. 943, 2014*

